Optica Applicata, Vol. XXV, No. 4, 1995

Hadamard spectrometer for luminescence emission measurements

A. CHRUŚCIŃSKA, H. L. OCZKOWSKI, K. PRZEGIĘTKA

Institute of Physics, Nicolaus Copernicus University, ul. Grudziądzka 5, 87–100 Toruń, Poland.

The basic problem encountered in measuring a weak luminescence spectrum is the optimum light gathering power. It is unfortunate that most systems use monochromator and scanning technique for recording spectra. The exit slit of a conventional scanning monochromator selects a small portion of dispersed radiation for detection. Since the whole light is extinguished, this method is extremely wasteful. This disadvantage may be overcome by using a multiplex technique in which an array of slits substitutes the one slit of monochromator. The optimum array corresponds to the Hadamard cyclic mask. For this reason, an optical assembly of a commercial monochromator (SPM1) was modified to Hadamard configuration. In this paper, the encoding arrangement with three masks of dimensions 255×0.1 mm, 63×0.3 mm and 63×0.1 mm, and the wavelength calibration procedure are described.

1. Introduction

When radiation is absorbed by a substance, some of its energy may be re-emitted as luminescence. In this context, radioluminescence (RL) is the emission of light from luminophors when nuclear radiation, such as alpha, beta of gamma rays, is incident on a material. Recently, most studies of luminescence phenomena have been connected with the photoluminescence (PL) and electroluminescence (EL) of semiconductors. The RL investigations concern mainly scintillators and solid state dosimetry.

Especially interesting for our laboratory is the "natural" thermoluminescence (TL) of minerals. The natural TL occurs due to exposure of the minerals to natural radioactivity. TL energy is accumulated by the minerals during the period of time which follows the last heating or bleaching. Taking data from the measurements of the accumulated ancient TL and the radioactivity of soil, it is possible to calculate the age of specimen. This is the principle of the thermoluminescence dating. On the other hand, it is possible to apply a recently produced pottery or brick as a natural dosemeter in case of accidental dosimetry [1]–[3].

It should be stressed here that the radioluminescence emission accompanies the excitation of thermoluminescence. Both phenomena are simultaneously excited by the same radiation events. Spectrum of RL depends on the type (alpha, beta, gamma) and intensity of nuclear radiation and on sample temperature. The emission bands of TL and RL characterize the active centres of radiative recombination. When the RL spectrum is compared with the temperature-resolved TL spectrum, a fundamental information about the nature of kinetic processes is attained.

In our previous paper [4], the high sensitivity spectrometer measuring the TL emission spectra by a multiplex Hadamard technique has been described in detail. In this spectrometer, we apply a variable, continuous interference filter as a dispersion element for the wavelength range from 400 nm to 765 nm, and 63 fields encoding mask. The detection system consists of the chopper for 77 Hz, photomultiplier with high output resistivity and the phase sensitive lock-in amplifier. Hence, at least in principle, this system works in direct current mode (d.c.) of signal detection. The absolute calibration shows that the low detection limit sufficient to record TL spectrum in 30 s, is about 10^8 photons/sr/s. This order of sensitivity corresponds to the intensity of light emitted from commercial EL diode powered by 5 μA.

The main problem of the TL spectrum measurement is that the TL emission is not only weak but has also transient character. Since it is much better to see something than nothing, the conflict between spectral resolution and detection sensitivity of TL is solved at the expense of spectral resolution. In practice, the spectral resolution of TL spectrometers is not higher than 5 nm [5]–[8].

Fortunately, the RL persists as long as one needs. Hence, even for weak excitation, the prolonged experiment allows a desirable singal-to-noise ratio (SNR) to be achieved. This makes it possible to apply a spectrometer of higher resolution in RL investigations. However, the d.c. mode of detection is inconsistent with the nature of RL. In the case of RL, one must record a spectrum of the luminescence emission composed of rarely and randomly distributed pulse events.

In any case, the measuring technique of RL should be similar to photon counting, *i.e.*, the detection system should involve pulse amplification, shaping and discrimination process. Taking into account the mechanism of the RL excitation by high energy photons and particles creating, in general, emission of more than one photon, the analysis of the pulse height of the luminescence events allows us to gain a deeper insight into the processes under investigation.

2. Hadamard spectrometry

The simplest method of spectral analysis is to use monochromator and scanning technique. But scanning technique suffers from serious disadvantage. Much of the dispersed light in the focus plane of spectrometer is rejected by an exit slit of monochromator. A multiplexed spectrometry offers here a simple remedy. Instead of one slit in the dispersion plane of spectrometer, a varying pattern of many slits is used. Thereby encoding mask enriches the brightness of spectrometer. In principle, a multislit mask performs the role of encoding arrangement of the multiplexing.

The multislit pattern of the mask forms an array of equidistant, open or closed slits. The total signal measured by a phototube behind encoding mask with defined pattern of slits is given by

$$y_i = \sum_j^N a_{ij} x_j \tag{1}$$

where $i = 1, 2, \ldots, N$ are pattern and measurement numbers, $j = 1, 2, \ldots, N$ are

numbers of the positions of equidistant spectral elements. Coefficient a_{ij} is either zero or one, respectively, for closed or open slit in the position j of spectral element. The binary array a_{ij} describes a veriety of patterns of encoding mask. For practical reasons, it is required that the matrix a_{ij} be cyclic. In this case, $2N-1$ equidistant elements of mask moving step by step along the window (N elements in width) yield N different patterns.

Proper array a_{ij} generates a set of linearly independent equations which allow calculation of the signal intensity corresponding to the position j of the spectrum

$$x_j = \sum_i^N b_{ij} y_i. \tag{2}$$

It has been shown that the optimum array of coefficients a_{ij} corresponds to the Hadamard simplex matrices and can be calculated for cyclic mask with $N = 2^n - 1$ elements, where n is a natural number [9], [10]. The following encoding pattern of cyclic mask has been calculated for our mask.

For $N = 63$:

1111110000 0100001100 0101001111 0100011100 1001011011 1011001101
010 (3)

and $N = 255$:

1111111100 1000010100 1111101010 1011100000 1100010101 1001100101
1111101111 0011011101 1100101010 0101000100 1011010001 1001110011
1100011011 0000100010 1110101111 0110111110 0001101001 1010110110
1010000010 0111011001 0010011000 0001110100 1000111000 1000000010
1100011110 10000 (4)

The decoding algorithm (2) is simple since

if $a_{ij} = 0$ then $b_{ij} = -2/(N+1)$, (5)
if $a_{ij} = 1$ then $b_{ij} = 2/(N+1)$. (6)

In the Hadamard encoding mask $(N+1)/2$ slits are open at the time and the measurements are repeated N times. Hence, in comparison with scanning technique, the value of SNR for Hadamard encoding is by $N^{1/2}/2$ higher.

3. Optical configuration

In our laboratories, a very popular Spiegelmonochromator 1 (SPM1) is supplied by Zeiss Jena. It consists of two concave mirrors ($\Phi = 53$ mm and $f = 352$ mm), plane mirror and prism as a dispersion element. SPM1 can be used with different exchangeable prisms (*e.g.*, quartz – Si68, glass – G60, UV NaCl), which cover a wide range of applications. Usually, the direct rectangular slit is used as an input and the curved slit as an output. Of course, a reverse direction is allowed. Precise micrometer drive with a scale T_0 rotates a prism and changes the transmitted

wavelength λ_0. The factory tables show the dependence $\lambda_0(T_0)$ for each type of prism In general, wavelength readout needs interpolation.

The images of curved slits are all sharp across the flat output plane and they have rectangular shape. Therefore, optical assembly of SPM1 has been modified to Hadamard configuration (Fig. 1). The encoding arrangement with three Hadamard cyclic masks ($m = B, C, D$) in the focal plane of SPM1 replaces the module of rectangular slit. Mask A consists of one rectangular slit and may be used during calibration. The arrangement allows quick and repeatable insertion of desired mask into fixed position of window.

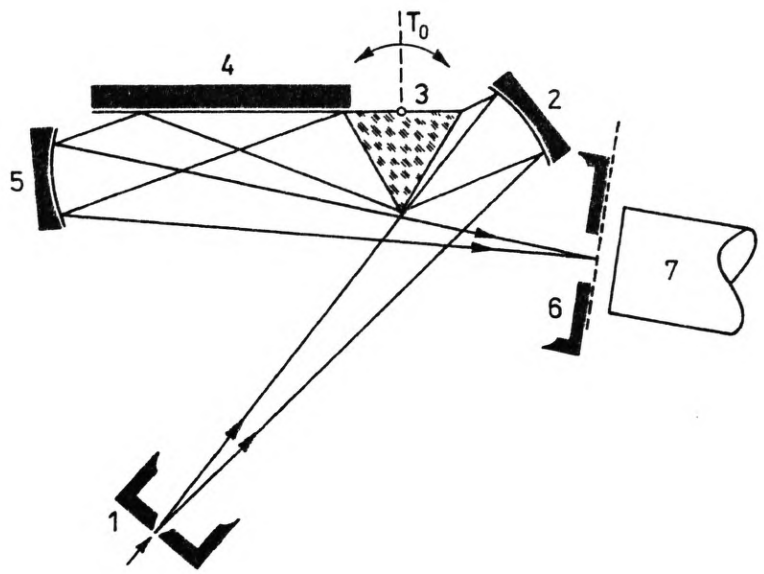

Fig. 1. Schematic diagram showing the optical assembly of SPM1 modified into the Hadamard spectrometer: 1 — curved input slit, 2 and 5 — concave mirrors ($\Phi = 53$ mm and $f = 352$ nm), 3 — prism, 4 — plane mirror, 6 — window and encoding mask, 7 — photomultiplier

Three encoding masks, placed one above another, have different patterns characterized by number N, the width of encoding elements d, and width of the window W. Symmetry axes of the windows fall into the position of the rectangular monochromator slit. Hence, the initial positions of narrower windows are shifted by a distance x_0 from the initial positions of the widest window. The parameters of the masks are given in Table 1.

Table 1. Dimensions of mask

m	N	d [mm]	W [mm]	x_0 [mm]
B	255	0.1	25.5	0
C	63	0.3	18.9	3.3
D	63	0.1	6.3	9.6

Encoding pattern of the masks corresponds to the binary array given by (3) and (4), respectively. The glass plate with the mask pattern is shifted by screw feeder of 0.3 mm pitch and stepper motor (72 steps/revolution).

4. Detection and control system

Dispersed and encoded light is detected by a cooled photomultiplier EMI 9203B with enhanced red response of trialkali photocathode (S20). The output cone angle of light transmitted by encoding mask is smaller than the effective cathode diameter (45 mm). The photomultiplier operates at negative high voltage (1200 V) with the anode at ground potential. Since the pulse counting technique is applied, a 50 ohm load impedance and the supplying capacitors (10 nF) are used in the last three stages of dynode chain. A simple pulse preamplifier (μA733 Fairchild) is located close to the photomultiplier anode. The output of the preamplifier is connected to a unipolar amplifier (4 μs mode) of the single channel analyser (SCA, window mode from 0.5 V to 9.9 V). The SCA produces output uniform pulses recorded by on-line computer After 3 hours of cooling down the count rate of dark pulses is about 100 s^{-1}.

In order to optimize the low threshold of the pulse discrimination, the entire spectrum of pulses from unipolar amplifier was measured by the pulse height multichannel analyser. Two successive counting runs, with and without the low intensity light, were performed. Experimental distribution of the pulse height at the output of amplifier is shown in Fig. 2. The spectrum of the background pulses *A*

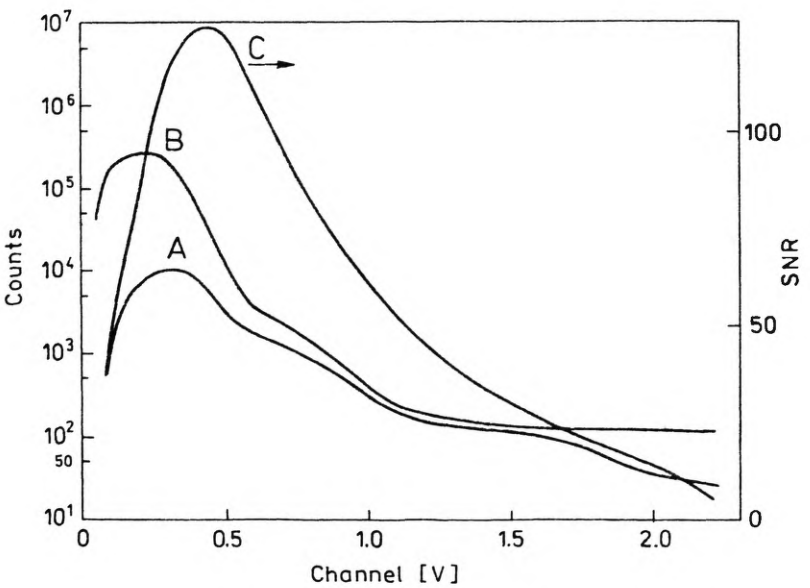

Fig. 2. Pulse-height analysis of pulses produced by the detector system (left scale — number of counts for 1000 s): *A* — dark pulses, *B* — number of additional pulses produced by light, *C* — SNR calculated from *A* and *B* (abscissa corresponds to the lower level discriminator)

and spectrum of the additional pulses produced by light B allows calculation of the dependence of SNR on the value of low level threshold of pulse selection C [11]. As a light source, the scintillator (SAD 12) excited by a weak laboratory alpha source (^{239}Pu) was applied in front of the entrance slit of the Hadamard spectrometer. The data collection time was 1000 s. The optimum value of low discriminator corresponds to the maximum of the SNR (0.5 V).

Measurements of the encoded signals are automated by using the PCL-718 multi-function data acquisition card for AT computer. Our application programme operates with QuickBasic 4.5 and uses software driver routines for PCL-718 accessed by the "call" statement from the driver library.

In this particular system, two features of the card are used – digital output channels and counter register. Two digital output channels control the unit of stepper motor, *i.e.*, "burst" pulse to switch on a group of pulses moving mask to the next position, and the second one, to reverse direction of the mask motion. The counter register counts photon events from the output of detection system (SCA). For each configuration of mask the recorded data are stored as a data file.

In the next part of programme, these data are decoded and can be manipulated in various ways. The direct method of decoding based on formulas (2), (5) and (6) is used.

5. Wavelength calibration

The encoding elements of mask divide the spectrum into equidistant N parts (fields). In the plane of dispersed spectrum the field position x for different masks m is given by

$$x = x_{0m} + p d_m \tag{7}$$

where $p = 1, 2, \ldots, N$ numbers of the positions of equidistant spectral elements. Since the value of T describes the linear dispersion of spectrum, then it is assumed that

$$T = Ax + B. \tag{8}$$

The value of T_0, read from the monochromator scale, corresponds to the central field of mask, or to $p = (N+1)/2$. Hence

$$T_0 = A\left(x_{0m} + \frac{(N+1)}{2} d_m\right) + B. \tag{9}$$

Finally, for the other fields of spectrum, expressions (7)–(9) can be written in the following convenient way

$$T - T_0 = a_m p - b_m \tag{10}$$

where

$$a_m = A d_m,$$

$$b_m = (N+1)Ad_m/2. \tag{11}$$

As already mentioned, the factory tables, and eventually the interpolation procedure give the dependence $\lambda(T)$. Therefore, for the purposes of wavelength calibration, the parameter A from (11) has to be estimated. For this reason, a spectral lamp HgCdZn (Philips), $T_0 = 650$ for quartz prism Si68, and the longest mask B (250×0.1 mm) were applied. With these parameters, a wide range of spectrum, from ultraviolet to near infrared, was covered. Decoded results for very strong Hg lines are shown in Table 2.

Table 2. Wavelength calibration – Hg lines

λ [nm]	$T(\lambda)$	p
404.7	666.0	120
434.7	633.8	140
546.1	556.7	183
579.1	542.1	192

From linear regression one can find the following expression for B mask

$$T_B - T_0 = 225.7 - 1.739p. \tag{12}$$

A small difference ($T - T_0 = -3.1$) which results from (12) for central element of the mask ($p = 128$) is close to the factory correction for the prism. In accordance with (10)–(12) for the C and D mask one can obtain

$$T_C - T_0 = 166.9 - 5.217p, \tag{13}$$

and

$$T_D - T_0 = 55.65 - 1.739p, \tag{14}$$

respectively.

These calibration formulas were applied for a wide spectral range. The measurements performed for different masks (C, D) and varying range of spectrum confirm the correctness of this method of wavelength calibration. The software for evaluation and graphical representation of encoded data is written in QB45. Interpolation subroutines from *Numerical Recipes* [12], [13] are incorporated.

6. Final remarks

The spectrometer SPM1 supplied by Zeiss Jena was originally designed for use as a scanning monochromator with different prisms. The basic concept of our modification consists in adopting the Hadamard multiplexed mode of spectrum recording. The result is similar to the spectral measurement performed by multichannel detector array, but Hadamard multiplex spectrometry allows only one photomultiplier detector to be used. Nowadays, photomultipliers are several times more sensitive than any other detector in the visible and near UV regions.

For our purpose, the choice of the SPM1 was clear since in this monochromator the slit unit is removable and the resulting aperture exposes the wide range of spectrum. The dispersion of the SPM1 (with quartz prism) is such that a spectrum extending from 300 nm to 1000 nm fills the largest encoding mask.

It should be noted here that at present the encoding patterns are made as a photomask on pyrex glass plate. Since the rectangular open slit, without any substrate, improves the mask transparence, then, in the future, the glass mask will be replaced by a metallic one.

The spectrometer system described here seems to the bright and flexible because the wavelength adjustment screw of SPM1, exchangeable prisms and masks make it possible to choose the desired range of spectrum. A computer control of measurements, simple algorithm for data and wavelength decoding display the results nearly on-line. Finally, it should be noted here that the Hadamard method allows the time-resolved spectra and multiphoton analysis to be performed by using the gate or pulse-height technique of data recording.

Acknowledgements— This work is supported by the State Committee for Scientific Research (KBN), project No. 2 P302 186 04.

References

[1] MCKEEVER S. W. S., *Thermoluminescence of Solids*, Cambridge University Press, Cambridge 1985.
[2] AITKEN M. J., *Thermoluminescence Dating*, Academic Press, London 1985.
[3] STONEHAM D., BAILIFF I. K., BRODSKI L., GOKSU Y., HASKELL E., HUTT G., JUNGNER H., NAGAMOTO T., Nucl. Tracks **21** (1993), 195.
[4] OCZKOWSKI H. L., Acta Phys. Pol. A **82** (1992), 367.
[5] BAILIFF I. K., MORRIS D. A., AITKEN M. J., J. Phys. E **10** (1977), 1156.
[6] JENSEN H. E., PRESCOTT J. R., PACT **6** (1982), 542.
[7] LUFF B. J., TOWNSEND P. D., Meas. Sci. Technol. **3** (1992), 65.
[8] TOWNSEND P. D., Radiat. Meas. **23** (1994), 341.
[9] NELSON E. D., FREDMAN M. L., J. Opt. Soc. Am. **60** (1970), 1664.
[10] HARWITT M., SLOANE N. J. A., *Hadamard Transform Optics*, Academic Press, New York 1979.
[11] COVA S., BERTOLACCINI M., BUSSOLATI C., Phys. Status Solidi A **18** (1973), 11.
[12] PRESS W. H., TEUKOLSKY S. A., VETTERLING W. T., FLANNERY B. P., *Numerical Recipes in Fortran. The Art of Scientific Computing*, Cambridge University Press, Cambridge 1992.
[13] SPROTT J. C., *Numerical Recipes Routines and Examples in Basic*, Cambridge University Press, Cambridge 1992.

Received September 14, 1995